# ISRG Journal of Engineering and Technology (ISRGJET)

OPEN ACCESS

**ISRG PUBLISHERS**

Abbreviated Key Title: ISRG J Eng Technol

**ISSN: 3107-5894 (Online)**

Journal homepage: https://isrgpublishers.com/isrgjet/

Volume – II Issue- V (September-October) 2026

Frequency: Bimonthly





## Harvesting Human Footstep Energy for Sustainable Electrical Power Generation and Storage Using a PZT-Based Piezoelectric Floor Tile


**Muhammad Zafar[1], Malik Muhammad Hamza[1], Saad Ur Rehman[1], Muhammad Zaheer[1], Tausif Ahmad[1], Muhammad Muneer[1*], Muhammad Sohaib Azeem[2]**

[1] Institute of Energy and Environmental Engineering, Faculty of Electrical, Energy and Environmental Engineering, University of the Punjab, Lahore, Pakistan

[2] School of Electrical and Power Engineering, Hohai University, Nanjing, China



| **Received:** 21-09-2026 | **Accepted:** 27-09-2026 | **Published:** 31-10-2026



***Corresponding author: Muhammad Muneer**



## Abstract

*This study presents the design, fabrication, and experimental characterization of a low-cost piezoelectric floor tile for converting intermittent human-footstep loading into electrical energy and delivering that energy through a complete conditioning and storage pathway. The prototype integrates thirty 27 mm lead-zirconate-titanate (PZT) discs in a 5-series × 6-parallel configuration on an 11 × 11 in. mechanical platform. The electrical output is processed through a full-wave bridge rectifier, a 1000 µF filter capacitor, and a buck–boost converter regulated to approximately 5 V before entering the downstream battery-protection/charging stage and 3.7 V lithium-ion storage. Under the reported laboratory loading conditions, output voltage increased from 8.2 to 20.0 V and current from 1.5 to 5.0 mA as the applied load increased from 20 to 60 kg, producing calculated electrical power from 12.3 to 100 mW. For the 0.0781 m² prototype footprint, the maximum calculated output corresponds to 1.28 W m⁻². The constant-load test showed a narrow voltage range of 19.8–20.1 V over 50 s. During a 100–1000 Ω resistance sweep, voltage increased while current decreased, with the highest calculated load power within the tested range occurring at 100 Ω. Battery-terminal voltage increased from 3.20 to 3.70 V during a 30 min repeated-excitation test. Surface-treatment experiments showed that graphite reduced calculated output power to 57.6 mW, whereas silver and RTV silicone produced approximately 100.5 and 97 mW, respectively. These results demonstrate the feasibility of integrating low-cost PZT transducers, mechanical force transfer, power electronics, energy storage, and a functional LED load in a single floor-tile platform. The study is positioned as a laboratory proof of concept; practical deployment will require calibrated pedestrian testing, energy-per-step measurements, conversion-efficiency analysis, long-term cycling, and field validation.*



**Keywords:** *piezoelectric energy harvesting; PZT; floor tile; human footsteps; energy harvesting interface; power conditioning; battery storage; low-power electronics.*



Copyright © ISRG Publishers. All rights Reserved.



**DOI: 10.5281/zenodo.23833951**

# 1. Introduction

Every human step represents a transient input of mechanical energy that is largely dissipated into the surrounding environment. In high-footfall environments, where pedestrian activity is continuous, this otherwise unutilized mechanical energy presents an opportunity for localized and sustainable electricity generation. The central engineering challenge in footstep energy harvesting, however, is not simply to produce a high instantaneous voltage; rather, it is to efficiently transfer the small and intermittent mechanical input through the transducer and power-conditioning circuitry while minimizing energy losses and maintaining mechanical reliability. Mechanical energy harvesting is particularly attractive for powering distributed, low-power electronics because the energy source is available directly at the point of use and can be converted without conventional fuel-based generation [28]. Among the available transduction technologies, piezoelectric conversion is particularly suited to footstep harvesting because mechanical stress or strain induces electrical charge within the piezoelectric material, enabling compact and structurally integrated generators for vibration, impact, and human-motion applications. [1–4]. Recent reviews have emphasized that practical performance depends not only on the piezoelectric material, but also on mechanical architecture, force transfer, electrical loading, and power-management circuitry [5–9].

Human footsteps are an especially interesting mechanical source because pedestrian movement repeatedly applies force to floors in transport terminals, commercial buildings, educational facilities, corridors, and other high-footfall environments. Reviews of piezoelectric floor tiles have shown a wide range of mechanical structures, transducer arrangements, and electrical interfaces, while also identifying low net energy per step, mechanical durability, force-transfer losses, and system economics as continuing challenges [1,2,10,30]. Experimental studies have demonstrated that pedestrian weight and walking conditions can substantially affect harvested energy, indicating that laboratory output cannot be transferred directly to field energy yield without accounting for realistic pedestrian behavior [2,4,14].

Recent work has moved toward more integrated systems. Selim et al. demonstrated a floor tile using piezoelectric patches for low-power applications, while Khajevand-Dalasmi and Jafari-Talookolaei experimentally investigated human walking on piezoelectric flooring [3,4]. A 2025 review further consolidated design strategies and product-development considerations for footstep energy harvesters [14]. Parallel research on footwear and human-motion harvesters has highlighted the importance of transducer arrangement, mechanical amplification, and application-specific power conditioning [15–18]. These studies collectively suggest that the most useful evaluation is system-level: the mechanical tile, piezoelectric array, rectifier, filter, voltage converter, storage element, and load should be considered as a connected energy pathway rather than as isolated components.

Electrical conditioning is particularly important because piezoelectric generators produce an alternating electrical response and exhibit source impedance that varies with operating conditions. Full-bridge rectification, DC–DC conversion, impedance matching, synchronous extraction, and maximum-power-point strategies have therefore received substantial attention [19–23]. Recent reviews show that even when a transducer produces a relatively high instantaneous voltage, poor electrical matching or conversion losses can substantially reduce useful energy delivered to a storage element or load [20–23].

Despite this progress, a practical gap remains between individual transducer demonstrations and low-cost floor-tile prototypes that combine array configuration, mechanical protection, power conditioning, energy storage, and experimental loading characterization [29]. The present work addresses this gap through a laboratory-scale prototype containing thirty commercial PZT discs arranged in a 5-series × 6-parallel topology. The study systematically examines load-dependent voltage, current, and power; short-duration voltage stability; electrical-load response; battery-terminal voltage during repeated excitation; area-normalized power; and the influence of surface coatings. The contribution is therefore not a claim of utility-scale generation, but an experimentally grounded assessment of an integrated, inexpensive footstep-energy harvesting pathway and the factors that govern its practical performance.

# 2. Materials and Methods

### 2.1 Prototype architecture

The prototype was constructed on an 11 × 11 in. (0.2794 × 0.2794 m) wooden platform with an active footprint of approximately 0.0781 m² as shown in Figure 1. A cushioning rubber/high-density foam structure was used above the base to distribute the applied mechanical load and reduce excessive local stress on individual discs. Thirty circular PZT discs, each 27 mm in diameter, were installed and electrically interconnected as five discs in series with six parallel branches. Series connection was used to increase the voltage capability of the array, whereas parallel branches increased the available current. The final configuration was selected as a practical compromise for the available number of discs and the intended low-power application.

| Parameter | Prototype value |
|---|---|
| Mechanical platform | 11 × 11 in. wooden board with rubber/foam force-transfer layers |
| Number of PZT discs | 30 |
| Disc diameter | 27 mm |
| Array configuration | 5 series × 6 parallel |
| Nominal array output | ≈20 V under the reported reference condition |
| Rectifier | Full-wave bridge |
| Filter capacitor | 1000 µF |
| DC–DC stage | Buck–boost converter, regulated to ≈5 V |
| Storage | 3.7 V rechargeable Li-ion battery with protection/charging stage |
| Demonstration load | LED array |
| Prototype active area | 0.0781 m² |

Table 1. Principal mechanical, electrical, and experimental parameters of the proposed piezoelectric floor-tile prototype.

Copyright © ISRG Publishers. All rights Reserved.
**DOI: 10.5281/zenodo.23833951**

### 2.2 Energy-conversion and conditioning pathway

Mechanical loading of the upper surface deformed the PZT discs and generated an AC electrical response through the direct piezoelectric effect. The array output was first passed through a full-wave bridge rectifier to obtain unidirectional electrical output. A 1000 µF capacitor was then used to reduce voltage fluctuations and smooth the rectified waveform. The conditioned signal was supplied to a buck–boost converter adjusted to approximately 5 V. The regulated output was connected to the downstream battery-protection/charging stage for the 3.7 V lithium-ion cell. Stored energy was subsequently demonstrated through an LED load. This architecture follows the general AC–DC–DC conditioning sequence identified in recent piezoelectric energy-harvesting interface studies [19–23].

| Circuit stage | Measured voltage | Function |
|---|---|---|
| PZT array | 20.0 V AC | Electrical generation from mechanical loading |
| After bridge rectifier | 18.7 V DC | AC-to-DC conversion |
| After 1000 µF capacitor | 18.9 V DC | Ripple reduction / energy buffering |
| After buck–boost converter | 5.0 V DC | Voltage regulation for downstream stage |
| Battery charging terminal | 5.0 V DC | Input to battery protection/charging stage |

Table 2. Measured voltage at successive stages of the power-conditioning pathway.

### 2.3 Experimental characterization

Characterization was performed under laboratory conditions using repeated manual compression/footstep loading. The principal loading sweep covered 20, 30, 40, 50, and 60 kg. Output voltage and current were measured at the electrical output of the array, and power was calculated from P = VI. The reported power-density values were obtained by normalizing calculated power to the fixed 0.0781 m² prototype footprint. A separate 50 s constant-load measurement was used to examine short-duration voltage stability, while a resistance sweep from 100 to 1000 Ω was used to observe the voltage–current trade-off under different electrical loading conditions. Battery-terminal voltage was monitored for 30 min during repeated excitation. Surface treatments were compared under comparable installation and loading conditions. Because the excitation was manually applied, the dataset characterizes the demonstrated laboratory operating points rather than a statistically sampled pedestrian population. Accordingly, the reported trends are interpreted as prototype-level relationships, and no generalized field-energy yield is inferred.

$$P = V I \quad \text{..... (1)}$$

where P is electrical power in watts, V is measured voltage in volts, and I is measured current in amperes. Power density was calculated from the measured electrical power divided by the fixed prototype footprint:

$$Pd = P / A \quad \text{..... (2)}$$

with A = 0.0781 m². The resistance sweep used 100, 220, 330, 470, 680, and 1000 Ω. A separate 50 s constant-load test was used to assess short-duration voltage stability. Battery-terminal voltage was monitored for 30 min during repeated excitation. Finally, three surface treatments, graphite, silver conductive paint, and RTV silicone—were compared with the uncoated PZT reference under comparable test conditions. Because the excitation was manually applied, the measurements represent the reported laboratory operating conditions and are not a statistical representation of a pedestrian population.

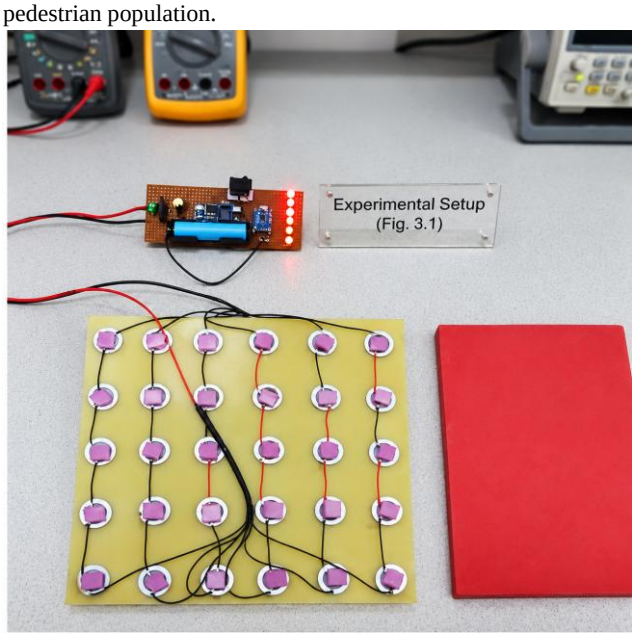



*Figure 1 Experimental Setup of the Proposed Piezoelectric Floor-Tile Prototype. The setup shows the piezoelectric disc array, electrical conditioning circuit, and mechanical top plate used for experimental testing of the prototype.*

## 3. Results and Discussion

The results are organized from transducer-level behavior to system-level behavior. First, the influence of mechanical load is established from voltage, current, and power measurements. The analysis then examines short-duration stability, electrical loading, battery response, area-normalized output, and surface protection. This sequence separates the intrinsic measured response of the prototype from the downstream effects of conditioning and storage.

### 3.1 Load-dependent voltage, current, and power

Figure 2 consolidates the four load-dependent measurements. The results show a consistent increase in electrical output as the applied mechanical load increased from 20 to 60 kg. In Figure 2(a), the measured output voltage increased from 8.2 V at 20 kg to 20.0 V at 60 kg, corresponding to a 143.9% increase. A linear fit to the five measured points gives a slope of approximately 0.295 V kg$^{-1}$ and $R^2$ = 0.996, indicating a strong empirical relationship over the tested range. The trend is physically plausible because greater applied force can increase deformation of the PZT elements and therefore the generated charge. However, the observed linearity is specific to this mechanical assembly and loading range; it should not be treated as a universal law for PZT floor tiles [1,5,8].

Figure 2(c) shows a corresponding increase in current from 1.5 mA to 5.0 mA. The increase of 3.5 mA represents approximately 233% growth across the tested load range. A linear fit gives approximately 0.088 mA kg$^{-1}$ with $R^2$ = 0.999. The strong

Copyright © ISRG Publishers. All rights Reserved.
**DOI: 10.5281/zenodo.23833951**

correlation indicates that the electrical array responded systematically to the increasing mechanical excitation under the selected configuration. Because the measured current depends on the electrical boundary condition, the current trend should be interpreted together with the load and voltage measurements rather than as an intrinsic current–force coefficient of the individual PZT material.

Figure 2(d) combines the voltage and current response through P = VI. The calculated power increased from 12.3 mW at 20 kg to 100 mW at 60 kg, a 713% increase. The increase in power is substantially larger in percentage terms than the voltage increase because both voltage and current rise simultaneously. A linear fit over the five points gives $R^2$ = 0.986, but the curvature of the measured values indicates that the power response is not perfectly linear. This distinction is important: the prototype demonstrates an increasing power trend with load, but it does not establish that power will continue increasing linearly at higher loads. Mechanical compliance, disc stress, displacement limits, contact conditions, and electrical loading would eventually constrain the response [5,24].

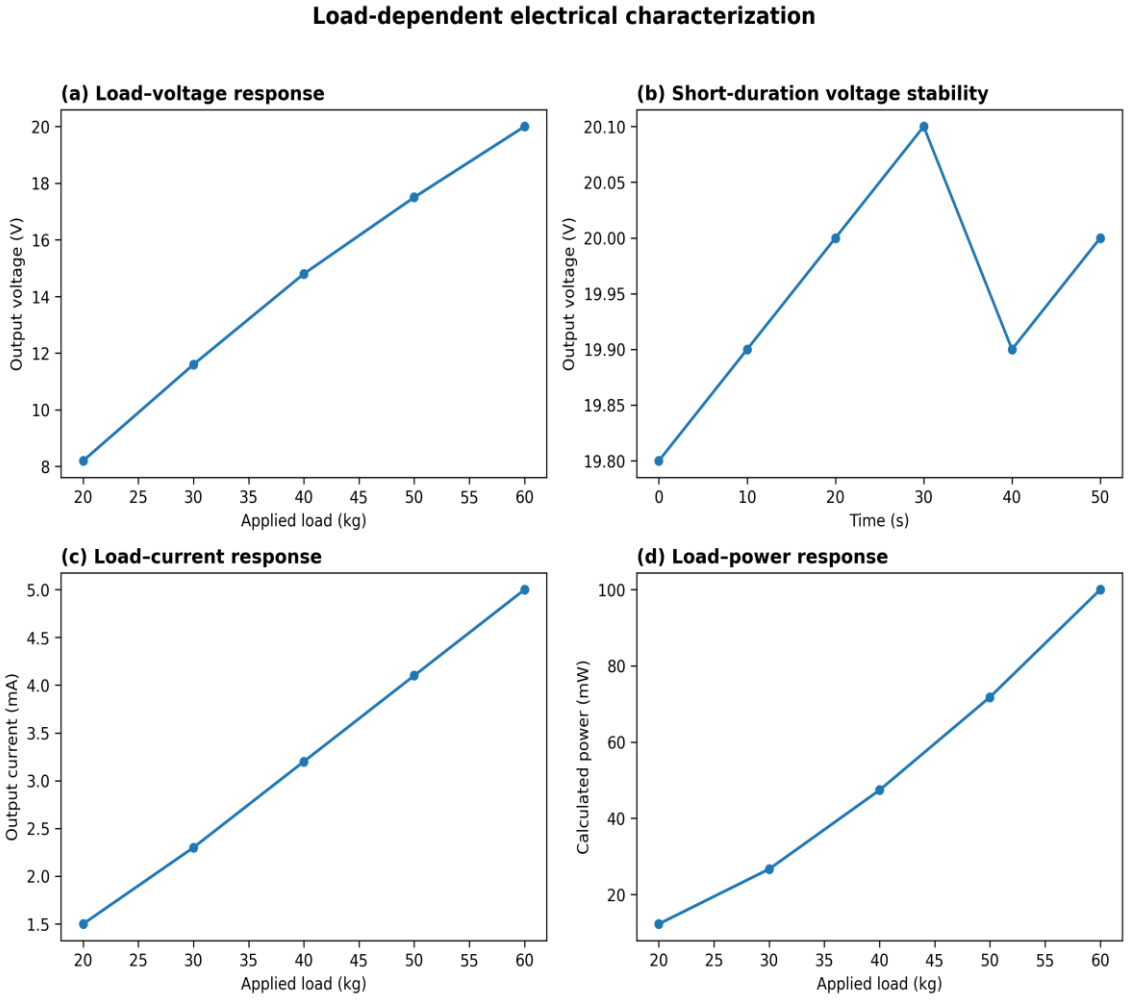



Figure 2. Load-dependent electrical response of the piezoelectric floor tile. (a) Output voltage versus applied load; (b) output voltage under constant loading versus time; (c) output current versus applied load; and (d) calculated electrical power versus applied load.

### 3.2 Short-duration voltage stability

Figure 2(b) presents the voltage response during the 50 s constant-load test. The measured values remained between 19.8 and 20.1 V, with a mean of 19.95 V and a sample coefficient of variation of approximately 0.53%. The narrow range indicates that the prototype could maintain a relatively stable measured voltage during this short laboratory interval when the mechanical condition was held approximately constant. However, this result should not be interpreted as evidence of long-term stability. Piezoelectric ceramics subjected to repeated mechanical cycling can exhibit fatigue-related degradation, and floor-tile systems also experience variability in force location, loading rate, temperature, mechanical wear, and assembly tolerances [24]. Long-duration cycling under controlled displacement and force should therefore be performed before claims of field durability are made.

### 3.3 Response to electrical load resistance

Figure 3(a) shows the electrical response as the external resistance was increased from 100 to 1000 Ω. Voltage increased from 15.8 to 20.0 V, while current decreased from 5.0 to 1.5 mA. This inverse voltage–current behavior is consistent with the expected response of a non-ideal voltage source whose operating point changes with load resistance. Importantly, voltage alone does not indicate the optimum operating condition for energy extraction. Calculating P = VI from the measured pairs gives approximately 79.0, 74.4, 65.9, 60.2, 44.9, and 30.0 mW for 100, 220, 330, 470, 680, and 1000 Ω, respectively. Thus, within the tested resistance range, the highest calculated load occurred at 100 Ω. This is a test-range observation rather than a definitive maximum-power-point determination, because resistances below 100 Ω and additional operating

Copyright © ISRG Publishers. All rights Reserved.
**DOI: 10.5281/zenodo.23833951**

conditions were not characterized. Recent interface-circuit literature emphasizes that impedance matching and load-dependent operation are central to maximizing useful, harvested power [19–23].

Figure 3(b) shows the battery-terminal voltage response during the 30 min storage test. The voltage increased from 3.20 to 3.70 V, corresponding to a 0.50 V or 15.6% increase relative to the initial terminal voltage. The result confirms that the harvested-energy pathway produced an observable change at the battery terminal during the reported experiment. Nevertheless, battery-terminal voltage alone is insufficient to determine charging efficiency, stored energy, state of charge, or coulombic efficiency. A rigorous charging assessment would require charging-current measurement, time integration of electrical power, battery state-of-charge characterization, and verification of the charger's constant-current/constant-voltage behavior. This limitation is particularly relevant for piezoelectric harvesters because the source is intermittent and the interface circuit must operate efficiently over a changing input condition [16,20–23].

Figure 3(c) shows the calculated power density, which increases from approximately 0.16 to 1.28 W $m^{-2}$ as calculated electrical power increases from 12.3 to 100 mW. Because the active area is fixed at 0.0781 $m^2$, this near-proportional relationship is mathematically expected from $P_d = P/A$. The 1.28 W $m^{-2}$ value should therefore be interpreted as an area-normalized output metric rather than as an independent efficiency measure. Comparisons with other harvesters should also account for differences in active area, loading mode, frequency, displacement, transducer type, conditioning circuit, and whether the reported value is instantaneous, average, peak, or RMS power [1,2,10].

Figure 3(d) compares the effect of surface treatment. The uncoated array produced approximately 20.0 V, 5.0 mA, and 100 mW under the reported reference condition. The graphite-treated configuration decreased output power to 57.6 mW, a reduction of 42.4%, while silver treatment produced approximately 100.5 mW and RTV silicone produced 97 mW. The graphite result indicates that a conductive coating is not automatically beneficial: the coating/binder layer may change mechanical compliance, stress transfer, surface contact, or electrical pathways. Because coating thickness, adhesion, and contact mechanics were not independently characterized, the exact mechanism cannot be established from the present measurements alone. The silver coating essentially preserved the reference performance, which is consistent with the fact that commercial piezoelectric discs already incorporate metallic electrodes. RTV silicone produced only a 3% reduction in calculated power while offering a plausible protective function, making it more relevant as a mechanical/environmental protection layer than as a performance-enhancing layer. These observations support the broader principle that packaging and surface engineering should be evaluated simultaneously for electrical and mechanical effects [8,12,14].

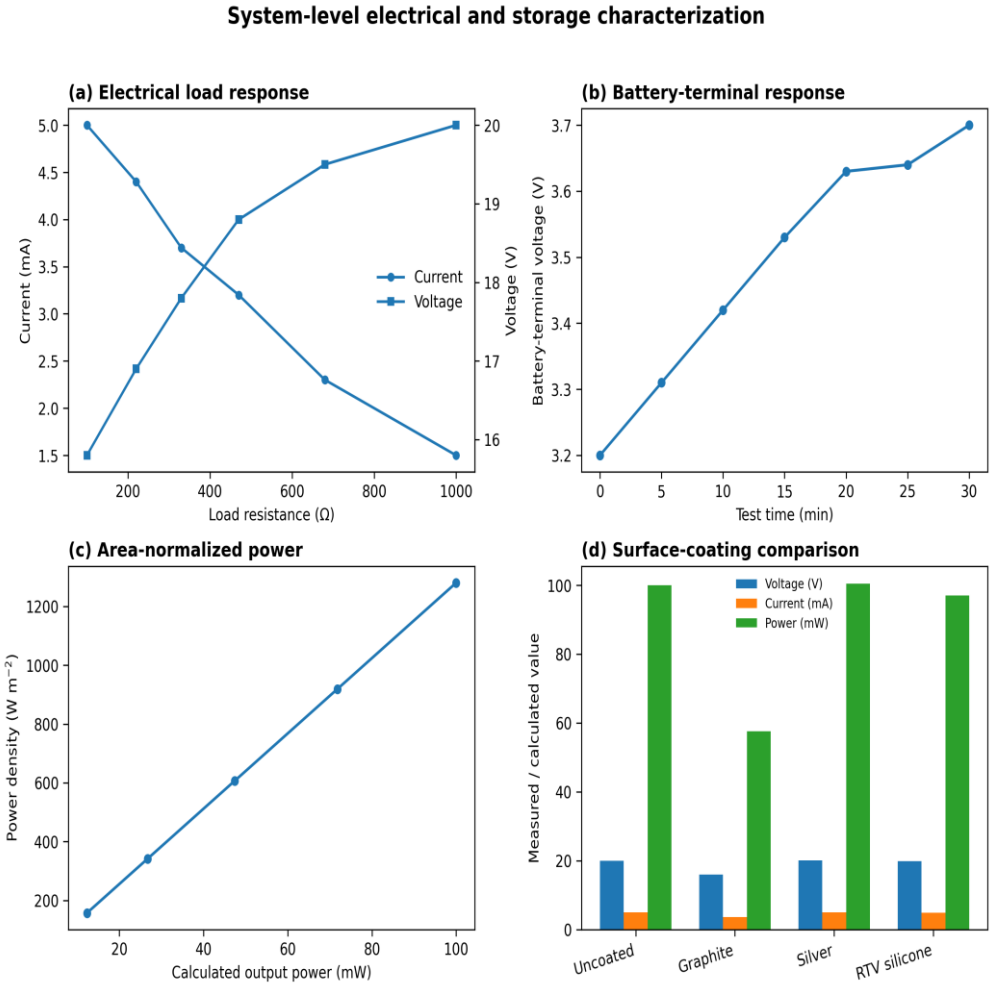



Figure 2. System-level electrical response of the prototype. (a) Voltage and current versus electrical load resistance; (b) battery-terminal voltage during 30 min of repeated excitation; (c) power density versus calculated electrical power; and (d) comparison of uncoated, graphite-coated, silver-coated, and RTV-silicone-coated configurations.

Copyright © ISRG Publishers. All rights Reserved.
**DOI: 10.5281/zenodo.23833951**

### 3.4 Power-conditioning pathway and functional demonstration

The measured conditioning stages provide a system-level view of how the generated AC signal was made compatible with storage and load operation. The array produced approximately 20.0 V AC under the reported reference condition, which became 18.7 V DC after full-wave rectification and 18.9 V after the 1000 µF filter capacitor. The buck–boost stage then produced approximately 5.0 V DC. The small increase from 18.7 to 18.9 V after the capacitor is consistent with the filtering/storage function of the capacitor under the measurement condition; it should not be interpreted as electrical energy gain. The final 5 V regulated output enabled connection to the battery-protection/charging stage and the LED demonstration. Recent reviews similarly identify rectification, voltage regulation, impedance matching, and energy-storage management as critical links between piezoelectric generation and practical loads [19–23].

The LED experiment provides a qualitative end-to-end demonstration: no footstep produced no visible output, a single compression produced a momentary response, and repeated loading produced brighter illumination as energy accumulated. This observation verifies the functional pathway from mechanical excitation to electrical output and storage/load operation, but it is not used here as a quantitative efficiency metric.

### 3.5 Comparison with recent literature

Table 3 places the present prototype alongside selected recent studies. Direct numerical comparison should be treated cautiously because published systems differ in transducer type, active area, mechanical amplification, excitation frequency, load definition, and whether the reported output is peak, RMS, instantaneous, or stored energy. Nevertheless, the literature shows that footstep harvesters are generally application-specific: some emphasize high instantaneous voltage, others maximize stored energy per step, and others optimize mechanical durability or electrical conditioning [1–4,10–18]. The present prototype contributes a low-cost integrated architecture with a clearly characterized load-dependent response and a complete conditioning/storage demonstration.

| Study | System / transducer | Reported focus | Relevance to present work |
|---|---|---|---|
| Yingyong et al. (2021) [2] | Piezoelectric floor-tile harvester | Pedestrians weight, pace, and harvested energy | Supports need for realistic loading conditions |
| Sharma et al. (2022) [1] | Piezoelectric floor tiles | Designs, circuits, feasibility, challenges | Provides floor-tile design context |
| Selim et al. (2024) [3] | Piezoelectric floor tile | Low-power floor-tile generation | Closest recent floor-tile comparison |
| Khajevand-Dalasmi & Jafari-Talookolaei (2025) [4] | Piezoelectric flooring | Experimental human-walking response | Supports human-loading characterization |
| Salleh et al. (2025) [14] | Footstep energy harvesters | Design strategies and product development | Recent system-level perspective |
| Gupta et al. (2023) [18] | Piezoelectric footwear | Walking/running and battery charging | Shows storage-oriented human-motion harvesting |
| Asadi et al. (2023) [12] | Electromagnetic floor tile | Footstep energy with frequency up-conversion | Contrasts of alternative transduction route |
| Present work | 30 PZT discs, 5S × 6P | 100 mW; 1.28 W $m^{-2}$; storage and LED demonstration | Integrated low-cost laboratory prototype |

Table 3. Selected recent studies relevant to footstep and human-motion energy harvesting. Reported metrics are not directly interchangeable because test conditions and definitions differ.

### 3.6 Practical implications and limitations

The measured maximum electrical output of 100 mW demonstrates that the prototype can produce useful low-power electrical energy under sufficiently high laboratory loading. However, the result should not be interpreted as continuous 100 mW generation from a pedestrian floor. Real-world output would depend on the number of footsteps, foot position, pedestrian mass, walking speed, duty cycle, mechanical displacement, force-transfer efficiency, electrical conversion losses, and storage efficiency [1,4,11,14]. The laboratory power-density value is therefore best viewed as a normalized characterization metric for comparing this particular prototype, not as a prediction of building-scale energy yield.

Several experimental limitations should be explicitly recognized. First, the loading was manually applied rather than generated by a calibrated force actuator with controlled displacement and frequency. Second, the dataset contains a small number of operating points and does not provide uncertainty bars or repeated statistical trials for every condition. Third, battery charging was assessed through terminal-voltage change rather than direct energy accounting. Fourth, long-term cycling and environmental exposure were not fully quantified. Finally, the PZT discs are lead-based ceramics, so future work should include environmental handling considerations and evaluate lead-free alternatives where practical [9,24,25].

Future optimization should therefore focus on calibrated force/frequency testing, mechanical impedance matching,

Copyright © ISRG Publishers. All rights Reserved.
**DOI: 10.5281/zenodo.23833951**

improved force distribution, a broader resistance sweep, direct measurement of rectifier and converter efficiency, controlled battery charging, repeated-cycle durability, and field trials under realistic pedestrian traffic. Advanced interface circuits such as synchronous extraction, adaptive rectification, and maximum-power-point control may also improve the fraction of generated energy delivered to storage [19–23].

## 4. Conclusion

A low-cost piezoelectric floor tile integrating thirty 27 mm PZT discs in a 5-series × 6-parallel arrangement was fabricated and experimentally characterized for footstep energy harvesting. The prototype exhibited a clear load-dependent response: output voltage increased from 8.2 to 20.0 V and current from 1.5 to 5.0 mA as the applied load increased from 20 to 60 kg, producing a calculated power increase from 12.3 to 100 mW. The 0.0781 $m^2$ active footprint corresponds to a maximum calculated power density of 1.28 W $m^{-2}$ under the reported laboratory condition. A 50 s constant-load test showed a narrow 19.8–20.1 V voltage range, while the electrical-resistance sweep demonstrated the expected trade-off between voltage and current and yielded a maximum calculated load power of 79 mW within the tested 100–1000 Ω range.

The integrated power-conditioning pathway converted the piezoelectric AC response through rectification, filtering, and DC–DC regulation to approximately 5 V, enabling a battery-storage demonstration and LED operation. The battery-terminal voltage increased from 3.20 to 3.70 V over 30 min; however, this voltage change should not be interpreted as a complete charging-efficiency measurement. Surface-treatment experiments showed that graphite substantially reduced output, while silver preserved the electrical response and RTV silicone caused only a small reduction, suggesting that RTV silicone may be more useful for protection than for electrical enhancement.

Overall, the results demonstrate the technical feasibility of an integrated PZT floor-tile energy harvester for low-power applications, but they also reinforce that practical deployment depends on mechanical durability, controlled force transfer, realistic pedestrian duty cycles, efficient power electronics, and rigorous energy accounting. The next stage should move from proof-of-concept characterization toward statistically repeated, calibrated, long-duration and field-based testing, with particular attention to energy-per-step, conversion efficiency, durability, and sustainable materials. The key experimentally demonstrated outcome is therefore an integrated 100 mW-class laboratory harvester rather than a claim of continuous building-scale power generation.

## References


1. Sharma, S., Kiran, R., Azad, P., & Vaish, R. (2022). A review of piezoelectric energy harvesting tiles: Available designs and future perspective. Energy Conversion and Management, 254, 115272. https://doi.org/10.1016/j.enconman.2022.115272
2. Yingyong, P., Thainiramit, P., Jayasvasti, S., Thanach-Issarasak, N., & Isarakorn, D. (2021). Evaluation of harvesting energy from pedestrians using piezoelectric floor tile energy harvester. Sensors and Actuators A: Physical, 331, 113035. https://doi.org/10.1016/j.sna.2021.113035
3. Selim, K. K., Yehia, H. M., & Saleeb, D. A. (2024). Energy harvesting floor tile using piezoelectric patches for low-power applications. Journal of Vibration Engineering & Technologies, 12, 8613–8622. https://doi.org/10.1007/s42417-024-01379-z
4. Khajevand-Dalasmi, M., & Jafari-Talookolaei, R.-A. (2025). Experimental investigation of energy harvesting from human walking on the piezoelectric flooring. Journal of Vibration Engineering & Technologies, 13. https://doi.org/10.1007/s42417-025-02104-0
5. Sezer, N., & Koç, M. (2021). A comprehensive review on the state-of-the-art of piezoelectric energy harvesting. Nano Energy, 80, 105567. https://doi.org/10.1016/j.nanoen.2020.105567
6. Sekhar, M. C., Veena, E., Kumar, N. S., Naidu, K. C. B., Mallikarjuna, A., & Basha, D. B. (2023). A review on piezoelectric materials and their applications. Crystal Research and Technology, 58, 2200130. https://doi.org/10.1002/crat.202200130
7. Brusa, E., Carrera, A., & Delprete, C. (2023). A review of piezoelectric energy harvesting: Materials, design, and readout circuits. Actuators, 12(12), 457. https://doi.org/10.3390/act12120457
8. Ali, A., Iqbal, S., & Chen, X. (2024). Recent advances in piezoelectric wearable energy harvesting based on human motion: Materials, design, and applications. Energy Strategy Reviews, 53, 101422. https://doi.org/10.1016/j.esr.2024.101422
9. Pan, X., Wu, Y., Wang, Y., Zhou, G., & Cai, H. (2024). Mechanical energy harvesting based on the piezoelectric materials: Recent advances and future perspectives. Chemical Engineering Journal, 497, 154249. https://doi.org/10.1016/j.cej.2024.154249
10. Zhao, B., Qian, F., Hatfield, A., Zuo, L., & Xu, T.-B. (2023). A review of piezoelectric footwear energy harvesters: Principles, methods, and applications. Sensors, 23(13), 5841. https://doi.org/10.3390/s23135841
11. Chandra, K. A., Narayan, S., Mamun, K. A., Chand, A. A., Prasad, D., & Ahmed, M. R. (2025). A review of footstep energy harvesting systems. IEEE Access, 13, 87149–87174. https://doi.org/10.1109/ACCESS.2025.3570963
12. Asadi, M., Ahmadi, R., & Abazari, A. M. (2023). Footstep-powered floor tile: Design and evaluation of an electromagnetic frequency up-converted energy harvesting system enhanced by a cylindrical Halbach array. Sustainable Energy Technologies and Assessments, 60, 103571. https://doi.org/10.1016/j.seta.2023.103571
13. Panthongsy, P., Isarakorn, D., Janphuang, P., & Hamamoto, K. (2018). Fabrication and evaluation of energy harvesting floor using piezoelectric frequency up-converting mechanism. Sensors and Actuators A: Physical, 279, 321–330. https://doi.org/10.1016/j.sna.2018.06.035
14. Salleh, M. M., Baharudin, N., Rohanai, R., Wagiman, K. R., Tamin, N., Abdul Rani, R., Ibrahim, A. N., Ghazal, M. H., & Azraai, M. N. (2025). Floor tile energy harvester: Design strategies, product development and performance analysis. ASEAN Engineering Journal, 15(2), 39–49. https://doi.org/10.11113/aej.v15.21944


Copyright © ISRG Publishers. All rights Reserved.
**DOI: 10.5281/zenodo.23833951**

15. Zhang, Y.-H., Lee, A., & Lee, C.-H. (2024). Design and application of piezoelectric and electromagnetic energy harvesters for mechanical energy harvesting in the human-body: A review. Sensors and Actuators A: Physical, 370, 115207. https://doi.org/10.1016/j.sna.2024.115207
16. Almarri, N., Chang, J., Song, W., Jiang, D., & Demosthenous, A. (2024). Piezoelectric energy harvesting and ultra-low-power management circuits for medical devices. Nano Energy, 131, 110196. https://doi.org/10.1016/j.nanoen.2024.110196
17. Ghandi, S., Al Janaideh, M., & Zhang, L. (2024). State of the art on power conditioning for piezoelectric energy harvesters. IEEE Transactions on Power Electronics, 39(3), 3724–3737. https://doi.org/10.1109/TPEL.2023.3345663
18. Gupta, S., Kumar, M., Singh, G., & Chanda, A. (2023). Development of a novel footwear based power harvesting system. e-Prime—Advances in Electrical Engineering, Electronics and Energy, 3, 100115. https://doi.org/10.1016/j.prime.2023.100115
19. Al Ghazi, A., Ouslimani, A., & Kasbari, A.-E. (2025). Advances in interface circuits for self-powered piezoelectric energy harvesting systems: A comprehensive review. Sensors, 25(13), 4029. https://doi.org/10.3390/s25134029
20. Yang, H., Huang, M., Ren, M., & Li, X. (2025). Piezoelectric energy harvesting interface circuit for small area and low power consumption—A review. Measurement, 242, 116051. https://doi.org/10.1016/j.measurement.2024.116051
21. Li, D., Wang, C., Cui, X., Chen, D., Fei, C., & Yang, Y. (2022). Recent progress and development of interface integrated circuits for piezoelectric energy harvesting. Nano Energy, 94, 106938. https://doi.org/10.1016/j.nanoen.2022.106938
22. Liu, H., Fu, H., Sun, L., Lee, C., & Yeatman, E. M. (2021). Hybrid energy harvesting technology: From materials, structural design, system integration to applications. Renewable and Sustainable Energy Reviews, 137, 110473. https://doi.org/10.1016/j.rser.2020.110473
23. Cai, M., et al. (2020). Fatigue in piezoelectric ceramic vibrational energy harvesting: A review. Applied Energy, 270, 115161. https://doi.org/10.1016/j.apenergy.2020.115161
24. Tiwari, B., Babu, T., & Choudhary, R. N. P. (2021). Piezoelectric lead zirconate titanate as an energy material: A review study. Materials Today: Proceedings, 43, 407–412. https://doi.org/10.1016/j.matpr.2020.11.692
25. Pham, T. H., Bui, T. D., & Dao, T. T. (2023). A high-reliability piezoelectric tile transducer for converting bridge vibration to electrical energy for smart transportation. Micromachines, 14(5), 1058. https://doi.org/10.3390/mi14051058
26. Bhorge, S., Kamble, D., Kandhare, S., & Sangameshwar, K. (2025). A piezoelectric-based platform for energy harvesting. In World Congress on Smart Computing, 41–52. https://doi.org/10.1007/978-981-97-9006-7_4
27. Covaci, C., & Gontean, A. (2020). Piezoelectric energy harvesting solutions: A review. Sensors, 20(12), 3512. https://doi.org/10.3390/s20123512.
28. Zafar, M., Hassan, S., Afzal, A., Muneer, M., & Azeem, M. S. (2026). Photocatalytic degradation of carcinogenic N-nitrosodiethylamine (NDEA) in amine-based $CO_2$ capture using carbon nitride under visible light. *ISRG Journal of Engineering and Technology*, *2*(3), 1–8. https://doi.org/10.5281/zenodo.20251168
29. Azeem, M. S., Abbas, T., Arshad, A., Muneer, M., Arif, B., Ali, S., & Zafar, M. (2025). Design and development of a small-scale composite vertical-axis wind turbine. *International Journal of Sustainable Applied Sciences*, *3*(8), 553–568. https://doi.org/10.59890/ijsas.v3i8.144
30. Azeem, M. S., Muneer, M., & Zafar, M. (2025). Development and performance evaluation of direct drive axial flux permanent magnet generator for small-scale wind turbines. *World Journal of Engineering*, 1–12. https://doi.org/10.1108/WJE-08-2025-0584

Copyright © ISRG Publishers. All rights Reserved.
**DOI: 10.5281/zenodo.23833951**